Development of Building Monitoring System to Evaluate Residual Seismic Capacity after an Earthquake

K. Kusunoki & A. Tasai
Yokohama National University, Yokohama

M. Teshigawara
Nagoya University, Nagoya

15 WCEE
LISBOA 2012

SUMMARY:
New residual seismic capacity evaluation system with inexpensive accelerometers is proposed. Response displacements are derived from measured accelerations by double integral with Wavelet Transform Method. The response of the measured building is simplified down to the single-degree-of-freedom system. The building for the department of architecture, Yokohama National University is instrumented the system since 2008. The health monitoring system worked well during the 2011 Off the pacific Coast of Tohoku Earthquake, too. The maximum acceleration was 91.5 cm/s^2 on the basement and 410 cm/s^2 on the roof. The predominant component of the acceleration lasted about 180 sec. In this paper, the evaluation results of the main shock such as the performance curve, stiffness degradation, and observed crack patters, and the histories of predominant periods and stiffness since 2009 when the building was retrofitted are discussed.

Keywords: Health Monitoring, Quick Inspection, Aftershocks, Tohoku Earthquake

1. INTRODUCTION

Due to Kobe Earthquake (1995, M7.3), 6,434 people were killed, and 104,906 buildings were totally collapsed. Maximum PGA of 848 gal was measured at Kobe Station of Japan Meteorological Agency. After that, number of sensor was drastically increased. Nowadays, there are more than 4,400 seismic intensity observation points (150 before Kobe Earthquake) and Kyoshin Net (K-Net) of NIED has about 1,000 strong motion observation stations in Japan.

After Kobe Earthquake, 17 large earthquakes occurred in Japan, which include Niigata Cyuetsu Earthquake (M7.2) in 2005 and 2011 Off the Pacific Coast of Tohoku Earthquake (M9.0). At the same time, a lot of earthquake ground motion data were measured by sensors. Some earthquakes caused severe damage of buildings and killed some people. Some earthquake, however, caused only slight damage to reinforced concrete structures although many earthquake records with large PGAs were measured.

JCI (Japan Concrete Institute) organized 'a research committee for seismic performance evaluation of reinforced concrete under recent earthquakes' and a report was published in 2004. The comparison of the earthquake records and observed damages in structures were made in the report and concluded that numerical analysis of records showed there must be but no buildings were observed severely damaged and monitoring building response is required to find out the reason of disagreement between analysis results and observations.

In order to promote building monitoring system, it must be attractive to owners. Therefore, a residual seismic capacity evaluation system with building monitoring system is proposed in this paper. Currently buildings have to be investigated one by one by engineers or researchers after an earthquake. For example, 5,068 engineers and 19 days were needed to investigate 46,000 buildings on a damaged area at the Kobe earthquake (BCJ 1996). Nineteen days were too long and yet the number of investigated buildings was not enough. Moreover, many buildings were judged as "Caution" level, which needs detailed investigation by engineers. "Caution" judgment is a gray zone and it could not take away anxieties from inhabitants. Furthermore, the current quick investigation system presents a dilemma since buildings should be investigated by visual observation of engineers. Thus, judgment varies according to engineers' experience. In order to solve these problems, building monitoring system is proposed in this research. The system has been installed to the building for Department of Architecture and Science in Yokohama National University in 2008, and the response during the 2011 Off the Pacific Coast of Tohoku Earthquake was successfully recorded. The damage of the building was evaluated from the response.

2. PERFORMANCE CURVE FROM MEASURED ACCELERATION

The performance curve is the relationship between the representative deformation Δ and the representative restoring force, which shows the predominant response of a structure. Non-linear response of multi-degree-of-freedom system is simplified down to a single-degree-of-freedom system with restoring force and deformation of Δ. The restoring force $\ddot{\Delta}$ is the base shear divided by the total mass of the building to change the unit to acceleration.

The configuration of the monitored building is shown in Fig. 2.1. Each floor basically has one accelerometer. If torsional response is expected, more than one accelerometer can be placed on a floor. In order to calculate inertia force, which is calculated as the mass multiplied by absolute acceleration, the mass of which response is represented by each accelerometer, m_i is needed. The summation of m_i is equal to the total mass of the building.

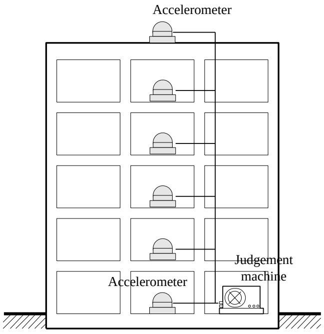

Figure 2.1. Configuration of the monitoring

The representative restoring force $\ddot{\Delta}$ and representative deformation Δ are calculated as Eqn. 2.1 and Eqn. 2.2, respectively [Kusunoki et al, 2008].

$$\ddot{\Delta} = \frac{\sum m_i \cdot \left({}_M\ddot{x}_i + \ddot{x}_0 \right)}{\sum m_i} \tag{2.1}$$

$$\Delta = \frac{\sum m_i \cdot {}_M x_i}{\sum m_i} \tag{2.2}$$

Where ${}_M\ddot{x}_i$ is i-th measured relative acceleration to the basement, $\ddot{x}_0$ is the ground acceleration measured at the basement, and ${}_M x_i$ is i-th relative displacement to the basement derived from the measured relative acceleration.

From Eqn. 2.1 and Eqn. 2.2, it can be said that m_i is not necessarily the absolute value but the relative to the total mass, which can be represented by the floor area governed by each accelerometer.

In order to decompose the acceleration and displacement into several components that have different Nyquist frequencies, the wavelet transform method (WTM) is applied as Eqn. 2.3 and Eqn. 2.4.

$$\left\{_M \ddot{x} + \ddot{x}_0\right\} = \left\{\sum_{i=1}^{N} g_{Accel,i} + f_{Accel,n}\right\} \tag{2.3}$$

$$\left\{_M x\right\} = \left\{\sum_{i=1}^{N} g_{Disp,i} + f_{Disp,n}\right\} \tag{2.4}$$

Where $g_{Accel,i}$ and $g_{Disp,i}$ are the i-th rank components of the absolute acceleration and relative displacement to the basement, and $f_{Accel,n}$ and $f_{Disp,n}$ are constant error values contained in the acceleration and relative displacement, respectively. The representative restoring force for the r-th rank $\ddot{\Delta}_r$ and the representative displacement for the r-th rank Δ_r are calculated as Eqn. 2.5 and Eqn. 2.6, respectively.

$$\ddot{\Delta}_r = \frac{\sum m_i \cdot_i g_{Accel,r}}{\sum m_i} \tag{2.5}$$

$$\Delta_r = \frac{\sum m_i \cdot_i g_{disp,r}}{\sum m_i} \tag{2.6}$$

If the i-th rank is not predominant, the performance curve of i-th rank shows meaningless relationship.

The displacement $g_{Disp,i}$ is calculated by the double integral of the acceleration $g_{Accel,i}$ with the conventional trapezoidal integral method. It is well-known that the double integral can give too large displacement because of the error component contained in the measured acceleration. Since the error component of the displacement has very long period, WTM can separate the error component from the predominant component [Kusunoki, et Al, 2008].

3. TARGET BUILDING

The proposed health monitoring system is installed into the building for the department of architecture of Yokohama National University in the beginning of the year of 2008. The building has 8 stories and 1 underground floor. The height of the building is 30.8m and its structural type is steel reinforced concrete. The building was designed before 1981, when the Japanese building code was revised to confirm the ultimate strength of buildings. It was found that the building did not have enough ultimate strength, and then the building was retrofitted. The retrofitting construction had been conducted from July 2008 to May 2009, and the sensors were removed at that time. The building before and after retrofitting is shown in Fig. 3.1. The key plan is shown in Fig. 3.2. EW direction is the longitudinal direction and NS direction is transverse direction.

After starting the monitoring, 112 earthquakes responses are measured until the 2011 Off the pacific Coast of Tohoku Earthquake, which occurred at 14:36, March 11th, 2011. After that, about 530 earthquake records are measured until the end of 2011.

(a) Before retrofitting (b) After retrofitting

Figure 3.1 Instrumented building

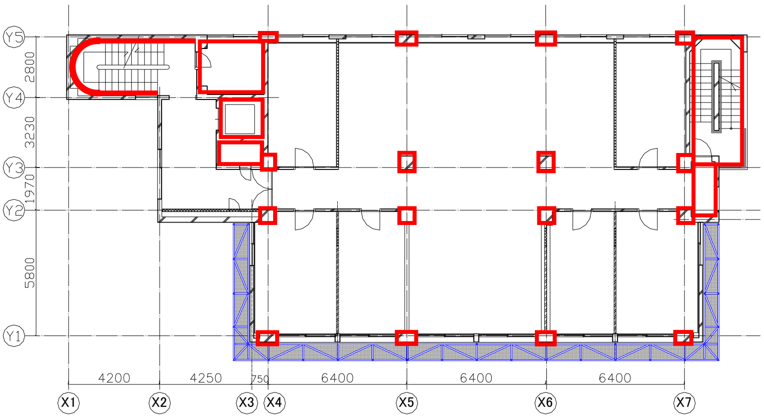

Figure 3.2 Key plan of the building

4. MEASURED RESPONSES

4.1. Responses during the Tohoku Earthquake

The health monitoring system worked well during the 2011 Off the pacific Coast of Tohoku Earthquake. Fig.4.1 shows the measured lateral accelerations on the basement and roof. The maximum acceleration was 91.5 cm/s^2 on the basement and 410 cm/s^2 on the roof. The predominant component of the acceleration lasted about 180 sec.

The measured performance curve, skeleton curve from the performance curve, and the demand curve in the EW direction are shown in Fig.4.2. The vertical axis of the demand curve is the response absolute acceleration spectrum Sa, and the horizontal axis is the response displacement spectrum Sd with viscous damping factor of 5%. The maximum representative displacement of 1.7cm was measured in the positive direction. The equivalent period from the maximum displacement point in the positive direction was 0.48 sec. The calculated viscous damping for the demand curve in order to get the same demand value for the period of 0.48 as the maximum response was 5.04%, which is reasonable value.

Since the natural period in the EW direction before the earthquake was about 0.41sec, the equivalent period of 0.48 is longer than the period before the earthquake. Fig.4.3 shows the skeleton curve and the slopes for the periods of 0.41sec and 0.48sec. It is clearly found that the stiffness degrading started at the representative acceleration of about 100cm/s^2. The stiffness degraded down to 73% according to the change of the period from 0.41sec to 0.48sec.

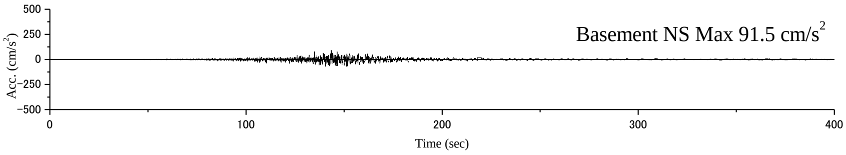

(a) NS direction on the basement

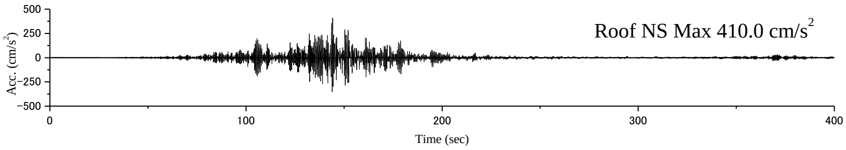

(b) NS direction on the roof

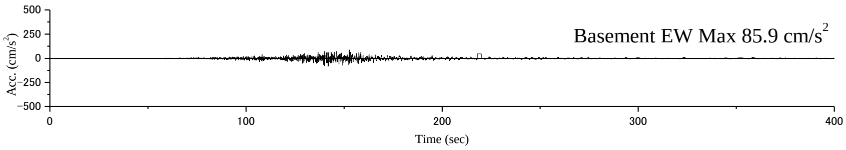

(c) EW direction on the basement

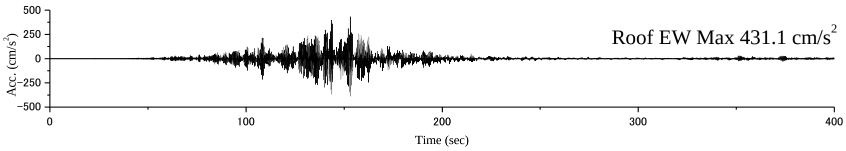

(d) EW direction on the roof

Figure 4.1 Measured earthquake during the 2011 Off the pacific Coast of Tohoku Earthquake

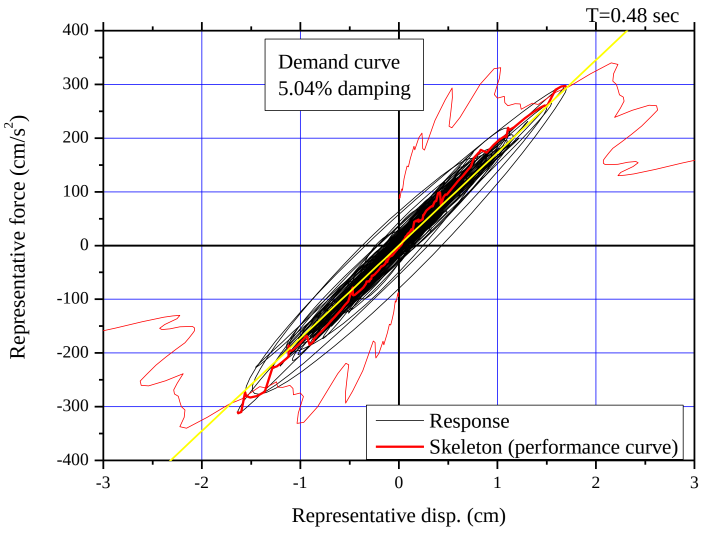

Figure 4.2 Measured performance and demand curves during the 2011 Off the pacific Coast of Tohoku Earthquake (EW direction)

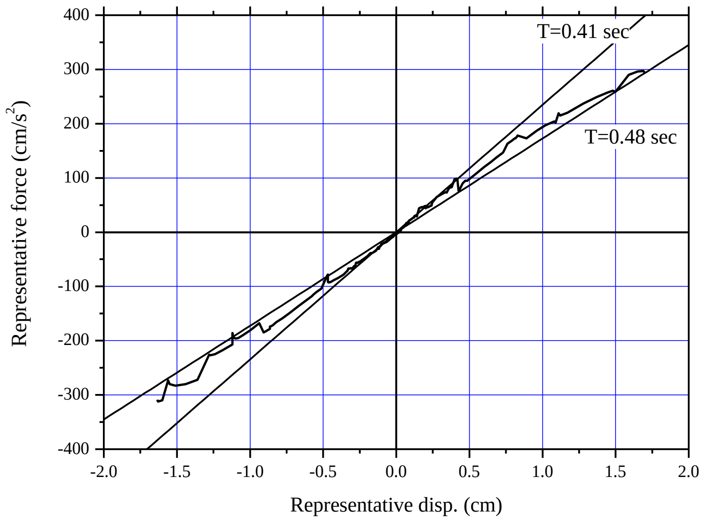

Figure 4.3 Skeleton curve of the measured performance during the 2011 Off the pacific Coast of Tohoku Earthquake (EW direction)

From Fig. 4.3, it can be said that the frequency change can be observed more accurately from the performance curve than from the transfer function, since the slope of the performance curve is square of the predominant angular frequency, ω. The transfer function sometimes does not show any predominant frequency if a large nonlinearity occurs during an earthquake. Moreover, while the performance curve shows the building has not yielded yet, it is unclear weather the damage is serious only from the frequency change.

Fig. 4.4 shows the relationship between the equivalent mass ratio (ratio of the equivalent mass to the total mass) and representative displacement. It can be said that the calculated equivalent mass ratio is stable even from very small displacement, and constant at about 0.77. The stable equivalent mass ratio can be an evidence to evaluate the proposed method worked successfully.

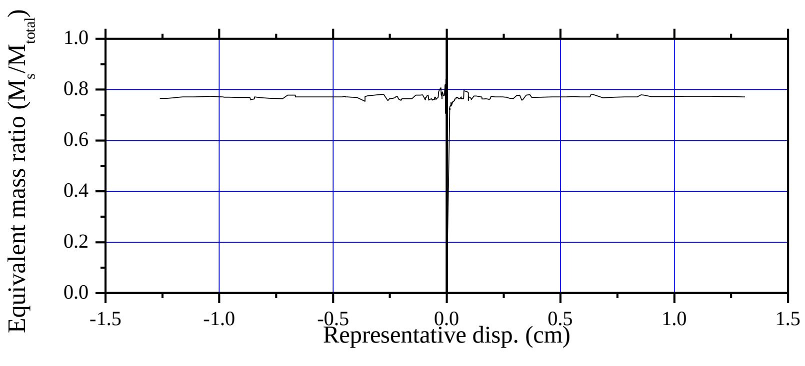

Figure 4.4 Equivalent mass ratio during the 2011 Off the pacific Coast of Tohoku Earthquake (EW direction)

After the main shock, cracks occurred in the building were investigated. The observed cracks in the Y3 frame are shown in the Fig. 4.5. Cracks occurred mainly at the bottom of the continuous shear walls and at the corner of openings. These cracks probably cause the stiffness degradation of the performance curve shown in Fig. 4.3.

The relationship between story shear force and inter-story drift can be calculated from the measured accelerations and calculated displacements. The relationships during the main shock are shown in Fig. 4.6. Equivalent stiffness of the relationship is calculated by the least square method and also shown as straight line in the figure. It can be seen that no significant degradation is observed, higher story contains more error, since inter-story drift of the higher story is smaller.

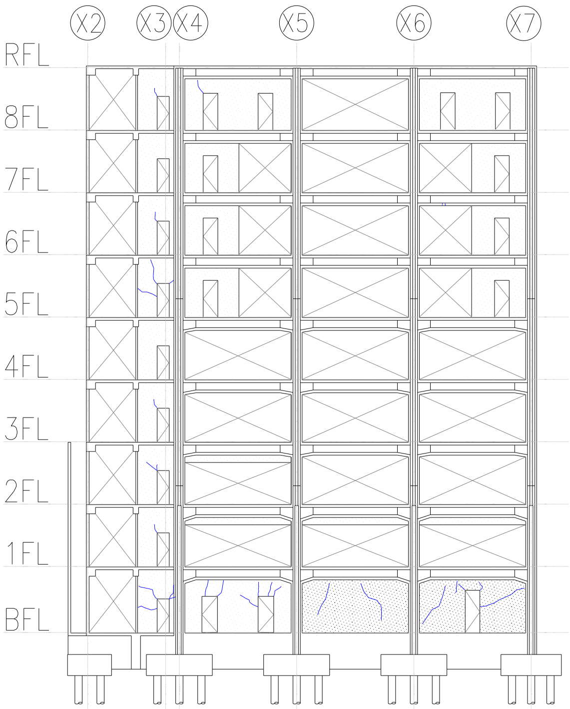

Figure 4.5 Observed cracks in the Y3 frame (EW direction)

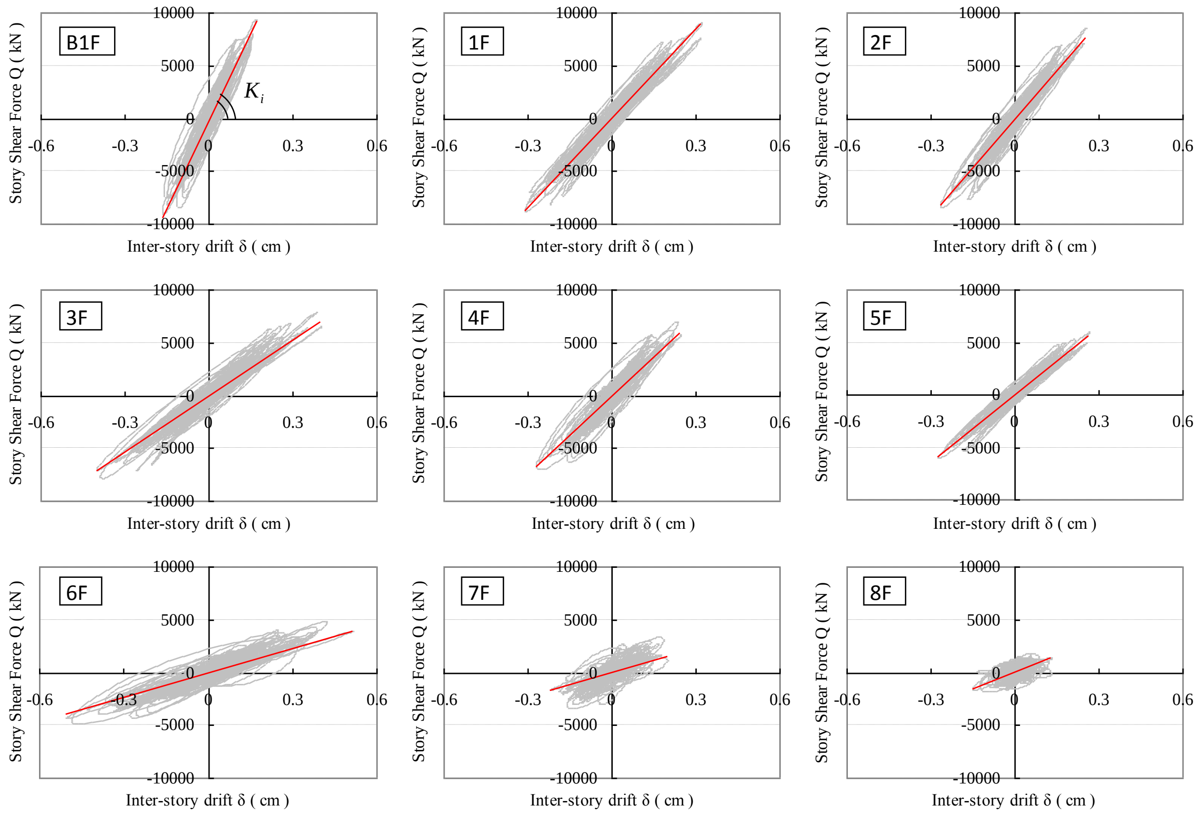

Figure 4.6 Relationship between story shear and inter-story drift (EW direction)

Eigenvalue analysis was conducted with the equivalent stiffness of each story shown in Fig. 4.6 and with the assumption that the masses of all stories are the same. The calculated first mode shape is shown in Fig. 4.7. The vibration shape at the maximum and minimum representative displacement of the performance curve can be considered as the "monitored" first mode, since the performance curve shown in Fig. 4.3 has only the first mode component. The monitored first mode shape is also shown in Fig. 4.7. Since the eigenvalue analysis result and monitored mode shape coincide very well, the equivalent stiffness shown in Fig. 4.6 represents story stiffness.

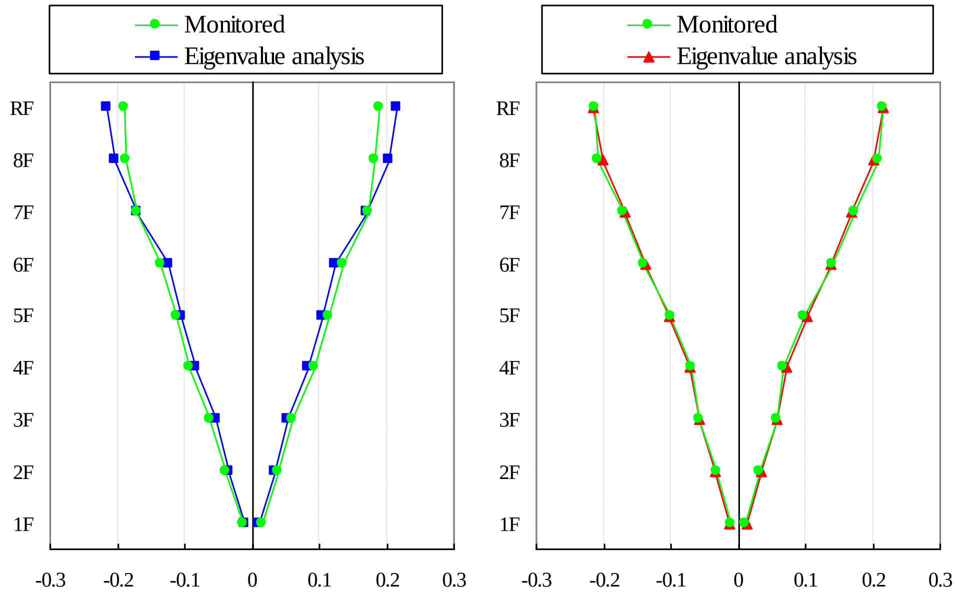

Figure 4.7 Comparison of the first mode shape between eigenvalue analysis and measurement

4.2. History of Predominant Period

Fig. 4.8 shows the history of the lateral period in both EW and NS directions from the beginning of the monitoring, Feb. 10, 2008 to Sep. 15, 2011. Periods had changed due to the retrofitting construction, where period became longer in the EW direction and shorter in the NS direction. After the 2011 Off the pacific Coast of Tohoku Earthquake, the periods in the both direction became longer due to the damage to the building as shown in Fig. 4.5.

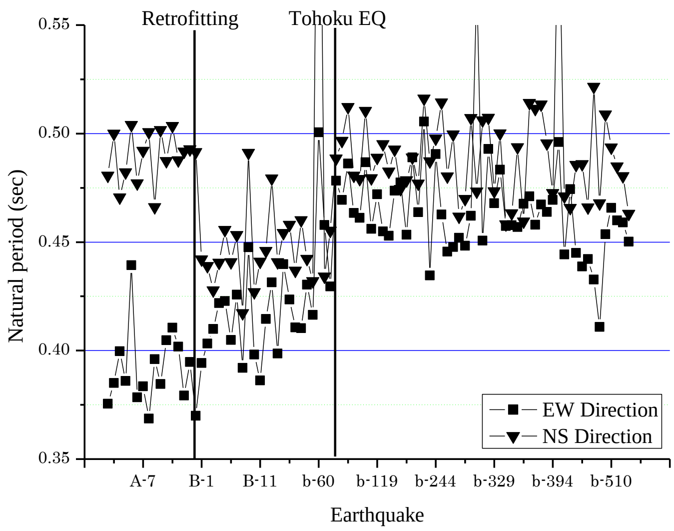

Figure 4.8 History of the lateral natural period

One of the advantages of the proposed method is that the representative force-displacement relationship can be obtained. If monitored response is evaluated only from the change of the period that is shown in Fig. 4.8, the ratio of the stiffness degrading is obtained that is 73% in this case. However, it is difficult to judge if the degradation of 73% means serious damage or not. On the other hand, the proposed method provides the force-displacement relationship as shown in Fig. 4.3. From the figure, it can be easily said that the stiffness degrading occurred due to cracking, not due to yielding, and the building may carry more lateral forces.

4.3. History of Story Stiffness

The relationships between story shear force and inter-story drift for all stories were calculated for records after retrofitting construction (2009) by the same method described in 4.1. The calculated equivalent stiffness for each story and record is shown in Fig. 4.9. The lower story has higher stiffness. Although the calculated stiffness scattered, it can be seen that the stiffness before the Tohoku Earthquake is almost constant. The stiffness, however, dropped down during the Tohoku earthquake. After the Tohoku Earthquake, the story stiffness is almost constant. Fig. 4.10 shows the PGAs of the recorded events after 2009. PGSs after the 2011 Off the pacific Coast of Tohoku Earthquake is less than 20gal. Therefore, further stiffness degradation did not occur after the main shock.

Looking at the stiffness of 8th story, stiffness contains error and becomes minus value for some records. As mentioned in 4.1, it is because the story drifts for the higher story is smaller, and then the effect of the error contained in the displacement effects more.

Fig. 4.11 shows the degradation ratio of the stiffness after the Tohoku Earthquake to the stiffness before the earthquake. The degradation ratio is almost the same for the all story as 80% except 8th story.

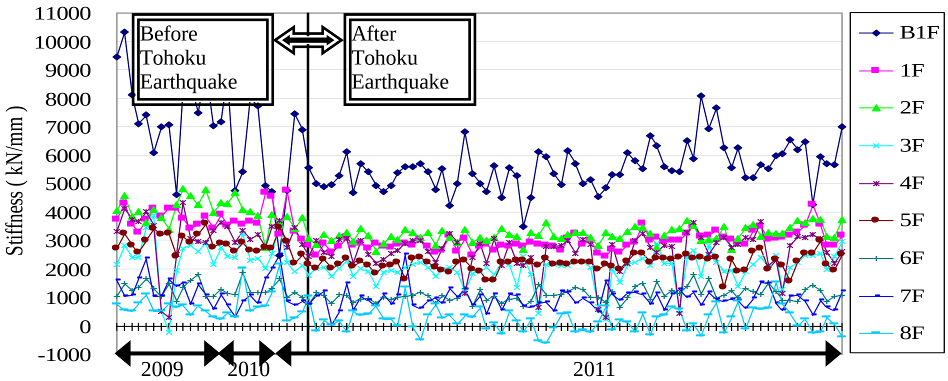

Figure 4.9 History of the lateral natural period

5. CONCLUDING REMARKS

A performance curve decomposition method using the Wavelet transform method was proposed to clear off the higher mode effects from a performance curve. The validity of the method was confirmed with the monitoring data of the building for the department of architecture of Yokohama National University including the record during the 2011 Off the pacific Coast of Tohoku Earthquake. Results from the studies are as follows;

- A performance curve decomposition method using Wavelet transform method was proposed.
- The developed WTM can efficiently decompose the dynamic response into its primary response frequency bands.

- In the investigated cases, the predominant performance curves of the building for the department of architecture of Yokohama National University were successfully extracted.
- The building suffered cracks during the 2011 Off the pacific Coast of Tohoku Earthquake and the degrading of the performance curve was successfully measured.
- The relationship between story shear force and inter-story drift is also derived from the record.

ACKNOWLEDGEMENT

Authors acknowledge Graduate Students Manabu Kawamura, Miho Yamashita, Daiki Hinata, and Yuuki Hattori for their great contributions to analyze records. The installation and maintenance of the measurement system has been supported by Mr. Masayuki Araki, Mr. Takamori Ito and other staffs of A Labo Co. Ltd. The research was partially supported by the Grant-in-Aid for Scientific Research (C).

REFERENCES

Kusunoki, K. and Teshigawara, M. (2004). Development of Real-Time Residual Seismic Capacity Evaluation System –Integral Method and Shaking Table Test With Plain Steel Frame-, *13th world conference on earthquake engineering*, CD-Rom.

Kusunoki, K., Elgamal, A., Teshigawara, M. and Conte, J. P. (2008). Evaluation of structural condition using Wavelet transforms, the 14th World Conference on Earthquake Engineering, CD-Rom

Kusunoki, K. and Teshigawara, M. (2003).A New Acceleration Integration Method to Develop A Real-Time Residual Seismic Capacity Evaluation System, *Journal of Structural And Construction Engineering*, No.569, 119-126 (in Japanese)

Percival. D. B. and Walden, A. T. (2002). Wavelet Methods for Time Series Analysis, Cambridge

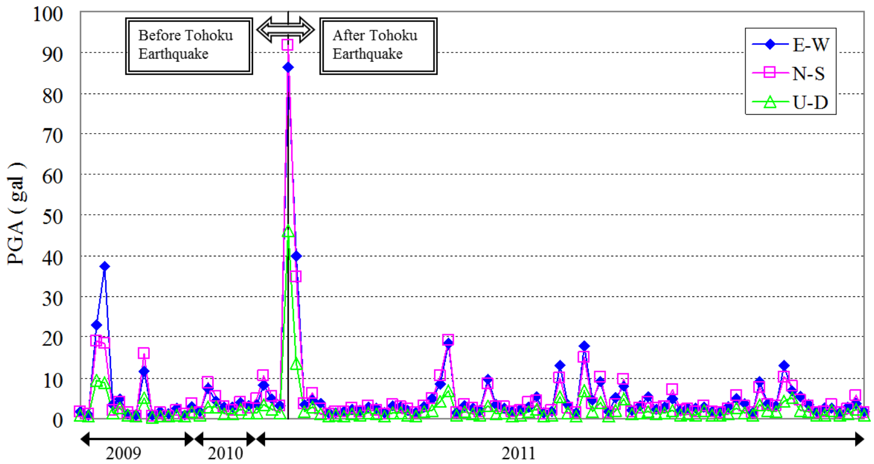

Figure 4.10 PGAs of the recorded events

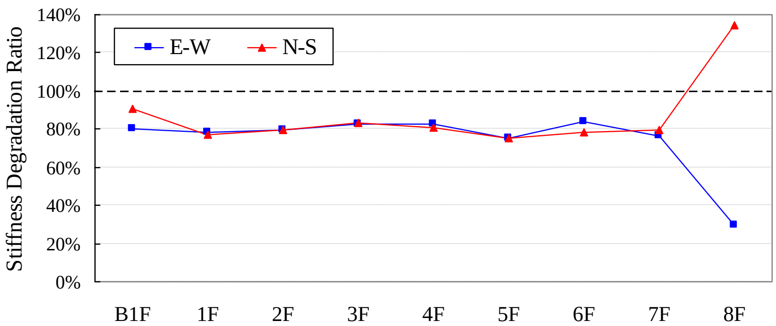

Figure 4.11 History of the lateral natural period